

August 2011

Boundary Value Problems in Geothermal Heat

Miguel Angel Rasco
Worcester Polytechnic Institute

Follow this and additional works at: <https://digitalcommons.wpi.edu/mqp-all>

Repository Citation

Rasco, M. A. (2011). *Boundary Value Problems in Geothermal Heat*. Retrieved from <https://digitalcommons.wpi.edu/mqp-all/1029>

This Unrestricted is brought to you for free and open access by the Major Qualifying Projects at Digital WPI. It has been accepted for inclusion in Major Qualifying Projects (All Years) by an authorized administrator of Digital WPI. For more information, please contact digitalwpi@wpi.edu.

Boundary Value Problems in Geothermal Heat

A Major Qualifying Project
submitted to the faculty of
Worcester Polytechnic Institute
in partial fulfillment of
the requirements for the degree of
Bachelor of Science

Submitted by:
Miguel A. Rasco, II, Mathematical Sciences

August 24, 2011

Advisor: Professor Burt S. Tilley

Abstract

In the rising technology of geothermal energy, a plant is only as good as the amount of heat it can extract from the ground. Understanding where heat is lost while it is being extracted from deep in the Earth is vital if the technology is to mature. This project proposes a mathematical model for a geothermal heat system in Germany with a staged production well and explores where heat is leaking from the well, and what can be done to avoid such losses in the future.

Acknowledgements

First and foremost, my sincerest thanks is given to my MQP advisor, Professor Burt Tilley, who never gave up on me as I worked through this project. Through the good and the bad, he was always an enthusiastic (not to mention patient) supporter of mine in ways that I didn't always deserve.

Additionally, the faculty and staff at Worcester Polytechnic Institute have always been never-ending sources of support and kinship ever since I arrived in "the Woo" 4 years ago. The experience has been exceptional, and one I won't soon forget.

Finally, my heartfelt gratitude and appreciation go to my family and friends (both within WPI and outside it). Without their love and support, I never would have been able to come as far as I have. This past academic year has been a most challenging one, and it is them who have gotten me through it, picking me up and pushing me forward whenever I stumbled.

To all of you, and more (you know who you are), I say "thank you".

Contents

1	Introduction and Background	3
1.1	Geothermal Heat	3
1.2	The Well	5
1.3	Derivation of the Heat Equation	6
1.3.1	Considering Conduction Through a Slice of a 1-D Rod	6
1.3.2	Looking at Multiple Dimensions	8
1.3.3	Examining Convection	9
1.4	Sturm-Liouville Theory	10
1.4.1	Definitions and Lagrange's Identity	10
1.4.2	Eigenvalues and Eigenfunctions	12
1.4.3	Singular Sturm-Liouville Problems	14
1.4.4	Method of Eigenfunction Expansion	16
2	Boundary Value Problem Derivation and Solution	17
2.1	Problem Development	17
2.1.1	Nondimensionalization	18
2.1.2	Separation of Variables	20
2.2	Finding the Basis Eigenfunctions	21
2.2.1	Finding the Basis Functions ϕ	21
2.2.2	Using Eigenfunction Expansion to Find Eigenvectors	22
2.2.3	Numerically Computing the Eigenvectors	22
2.3	Solving for the Nondimensional Θ	23
3	Results	26
3.1	Temperature Rise in Each Mode	26
3.2	Variation of the Péclet Number	28
4	Conclusions	30
4.1	Applying our Results	30
4.2	Future Work	30
A	Matlab Source Code	33
A.1	eigens.m	33
A.2	nondim.m	34

Chapter 1

Introduction and Background

In the ever-expanding global economy, the issue of energy is unescapable. Questions like “How can we use it?”, “How can we harvest it?”, and “Where can we get it?” are the primary concerns of those in this field. With the limited supply of petroleum and the rising expense of safely harvesting it, the world is increasingly looking to nature for replacements that are cleaner, safer, and cheaper. Over the years, technologies for gathering solar, wind, and nuclear power have matured and been implemented all over, from the third world to the first. Looking to the Earth itself is the next logical step for finding renewable energy. This project is one that is primarily concerned with the production of geothermal energy, and the journey it takes from the Earth’s interior to its surface.

1.1 Geothermal Heat

Geothermal energy is one that is generated by heat within the earth. The earth’s interior is heated by radiation from the decay of elements such as uranium and potassium in the crust and mantle. The flow of this heat isn’t uniform throughout the earth and, as such, certain areas offer greater potential for harvesting this energy than others. Fluid transport via wells to and from the earth’s surface is the primary method for utilizing geothermal energy, and there are three types of systems of geothermal energy. In hydrothermal systems, convection is used to move water and/or steam into and out of the interior of the earth. In geopressed systems, heat is generated through the dissolution of methane under intense pressure from sediment and rock above it. Hot dry rock systems require the introduction of a fluid to extract heat and bring it to the surface. Among these three, hydrothermal systems are the easiest to extract heat from and have proven themselves over time as reliable sources of geothermal heat.[4]

Geothermal energy has been mined and exploited since the Roman Empire,

yet it wasn't until the past few decades that its true potential as a generator of electricity was realized. The first generator that ran on steam emanating from the earth was built in Italy in 1904. Soon, other countries caught on to the new technology and emulated it with their own power plants. However, like many other natural energy resources (e.g. fossil fuels), geothermal energy currently available for harvesting is neither new nor readily renewable. Due to the relatively quick harvesting rate (vs. the slower natural input rate), the lifespan of a tapped geothermal reservoir can be significantly limited and shorter than that of an untapped reservoir.[5]

While hydrothermal energy mined from the earth's geothermal basins has many advantages to it, there is a large potential for energy contained in so-called hot dry rocks. These resources, as one would expect, do not contain any moisture naturally and as such the energy they contain is much more difficult to harvest than that of a hydrothermal source. However, their abundance is much greater around the world. Currently known limitations and vulnerabilities to these resources present some inhibition to their potential with current technology. However, in the coming years, new technology should be able to overcome these obstacles and tap the energy in hot dry rocks to their full potential.[5]

Figure 1.1.1 shows a typical setup for a geothermal heat system. Basically, a production well (shown on the right in the figure) is drilled deep enough to tap into a supply of groundwater beneath the surface. This water is then pushed to the surface through these wells by the Earth's geological processes. Depending on the resource being tapped, the temperature of the water brought to the surface can vary anywhere from 150 °C upwards of 300 °C. Depending on the amount of pressure the water is under, it can come up as either a liquid or steam. From there, the water is sent to a power plant where it can produce electricity or serve some other purpose.[6]

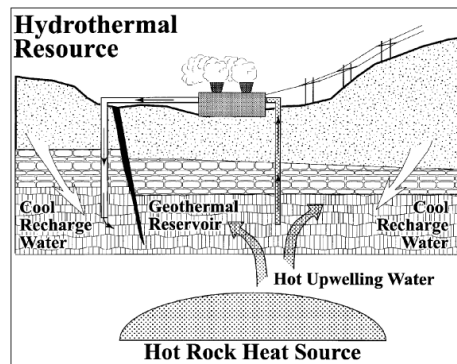


Figure 1.1.1: Diagram of a typical geothermal heat system.[6]

While geothermal energy has several advantages over other forms of energy, it is not without disadvantages. Since the groundwater being tapped is coming from several kilometers below sea level, it comes up with impurities. Depend-

ing on the harvest site, the composition and concentration of the water varies. While some substances found in the water are relatively benign at relatively low temperatures (around 100 °C), other substances such as sodium chloride, bicarbonate, and silica can be more harmful at higher temperatures (200 °C - 360 °C). The amount of heat this water is exposed to can cause the substances within it to be corrosive and cause damage to well lining and surface equipment. While modern technology doesn't allow this corrosivity to stand in the way developing geothermal heat, it is limited by it. However, the challenges presented by impure groundwater make the production of geothermal heat more expensive than it could be, and work to counteract these adverse effects is well underway.[6]

1.2 The Well

The goal of this project centers around a geothermal heat plant in Pullach, a German town that shares a border with Munich. Operated by *Innovative Energie für Pullach*, it is charged with providing heat for the small town of 8,733.[2] Figure 1.2.1 shows a detailed view of the production well in question (l) as well as a general diagram of the plant (r).

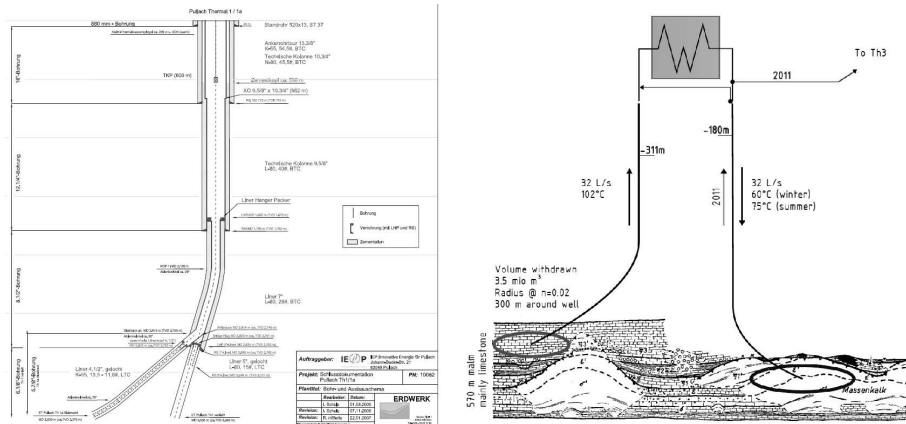


Figure 1.2.1: Diagrams of the well in Pullach, Germany

It is the journey of the water up the production well that is of interest. As one would expect, the water is cooler once it reaches the surface than it was when it first entered the pipe. How much cooler is known. How it cools off, and where in the well this cooling takes place, however, is not, and that is the focus of this project. By applying the physical properties of the well and the water is transports to a well-known differential equation, we will construct a mathematical model of the temperature of the water from beginning to end. This model will help map for us where temperature loss is taking place, and what may be causing those losses.

1.3 Derivation of the Heat Equation

On a fundamental level, this project is primarily concerned with heat transfer in a vertical pipe. To begin construction of our desired model, we must first derive a differential equation for heat transfer. In the simplest sense, we treat the fluid in the pipe as a one dimensional rod of uniform width and length L . Figure 1.3.1 gives a graphic representation of the rod.

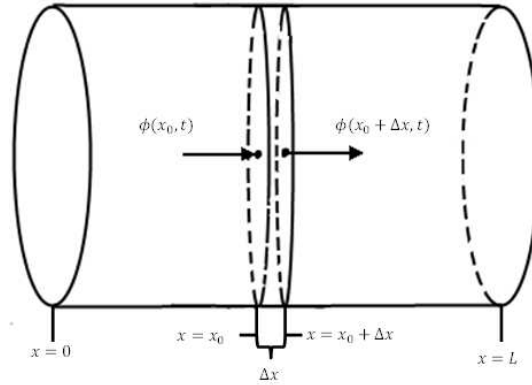


Figure 1.3.1: Diagram of 1-dimensional rod with heat flowing through a slice of width Δx .

1.3.1 Considering Conduction Through a Slice of a 1-D Rod

We will examine heat flow through the small slice of the rod illustrated above. Table 1.3.1 describes physical properties of the pipe and rod as well as the representative variables of those properties.

Property	Representative variable
Heat flux through the point x at time t	$\phi(x, t)$
Cross-sectional area of the pipe and slice	A
Temperature at point x at time t	$u(x, t)$
Specific heat at x	$c(x)$
Density at x	$\rho(x)$

Table 1.3.1: Physical properties of the pipe

Typically, specific heat and density are considered to be uniform (constant) throughout the pipe, but in general they can vary according to position.

To quantify the heat energy flowing through the designated slice of the, we examine the pipe's physical properties, and derive energy from what we know.

To that end, heat energy (designated “ $H.E.$ ”), is given by

$$H.E. = \rho(x)c(x)u(x, t)A\Delta x. \quad (1.3.1)$$

If we examine the units on the right-hand side of (1.3.1), we see that

$$\text{energy} = \frac{\text{mass}}{\text{volume}} \times \frac{\text{energy}}{\text{mass} \times \text{degrees}} \times \text{degrees} \times \text{volume}$$

which verifies the equation given for $H.E.$ We then apply the fundamental principle of conservation of energy (in this case, heat energy), to analyze further the energy flow through the slice. The principle states that any change in temperature over time is due to heat flow across boundaries (in this case, $x = x_0$ and $x = x_0 + \Delta x$) and any heat generated within the rod. The latter quantity can be expressed in terms of a new variable, $Q(x, t)$, which gives the rate of heat energy generated per unit of volume. In terms of units, Q is given by

$$Q(x, t) = \frac{\text{energy}}{\text{volume} \times \text{time}}.$$

For this slice, the principle of conservation of heat energy can be mathematically expressed as

$$\frac{\partial H.E.}{\partial t} \approx A[\phi(x, t) - \phi(x + \Delta x, t)] + Q(x, t)A\Delta x. \quad (1.3.2)$$

Since we have an explicit definition of $H.E.$, however, the left-hand side of (1.3.2) can be written as

$$\frac{\partial H.E.}{\partial t} = \rho(x)c(x)A\Delta x \frac{\partial u}{\partial t} \quad (1.3.3)$$

since x is fixed and ρ and c do not depend on t .

The equation in (1.3.2) is given only as an approximation since some quantities are assumed to be constant and/or fixed in our slice. We can refine (1.3.2), however, if we consider the case where Δx becomes infinitely small. To avoid a trivial $0 = 0$, we first divide (1.3.2) by Δx (after substituting in (1.3.3)) before applying our limit. This gives us

$$\rho(x)c(x) \frac{\partial u}{\partial t} = \lim_{\Delta x \rightarrow 0} \frac{\phi(x, t) - \phi(x + \Delta x, t)}{\Delta x} + Q(x, t) \quad (1.3.4)$$

or, equivalently,

$$\rho(x)c(x) \frac{\partial u}{\partial t} = -\frac{\partial \phi}{\partial x} + Q(x, t). \quad (1.3.5)$$

Note the use of equality and the fact that A was canceled out. Equation (1.3.5) can be alternatively derived over a larger region of the rod using more general boundaries $x = a$ and $x = b$ and the fundamental theorem of calculus over the flux between a and b .

We now turn our attention to Fourier’s law of conductivity to complete our derivation of the heat equation. The following properties of heat flow in general serve as a premise to the law:

1. No energy flows if temperature in a medium is constant.
2. If temperature is not constant or uniform, heat energy flows from warmer regions to cooler regions.
3. Heat energy flow rate is directly proportional to temperature difference.
4. Different materials generate varying rates of heat energy flow (even if temperature differences are consistent between the materials).

Mathematician Joseph Fourier experimented with these properties and came up with the formula

$$\phi(x, t) = -K_0 \frac{\partial u}{\partial x} \quad (1.3.6)$$

known as Fourier's law of conductivity.[3] The constant K_0 illustrates property 4 and is known as the thermal conductivity constant of the material in question. The minus sign in (1.3.6) illustrates property 2 since an increase in temperature to the right (i.e. as x increases) results in great heat energy flow to the left (i.e. as x decreases).

If we substitute the definition heat flux given in (1.3.6) into the principle of conservation of heat energy given in (1.3.5), we arrive at the partial differential equation

$$\rho(x)c(x) \frac{\partial u}{\partial t} = -\frac{\partial}{\partial x} \left(-K_0 \frac{\partial u}{\partial x} \right) + Q(x, t). \quad (1.3.7)$$

In this model, we are assuming that the material in the rod is uniform, so $\rho(x)$, $c(x)$ and K_0 may all be assumed to be constant. Therefore, (1.3.7) can be rewritten as

$$\rho c \frac{\partial u}{\partial t} = K_0 \frac{\partial^2 u}{\partial x^2} + Q(x, t). \quad (1.3.8)$$

If there are no sources of heat external to our slice (i.e. $Q \equiv 0$), then we can divide by the constant ρc to give us

$$\frac{\partial u}{\partial t} = \kappa \frac{\partial^2 u}{\partial x^2} \quad (1.3.9)$$

where

$$\kappa = \frac{K_0}{\rho c}.$$

Equation (1.3.9) is known as the heat equation.

1.3.2 Looking at Multiple Dimensions

The heat equation given by (1.3.9) works if the medium being considered is one-dimensional and uniform. In general, however, we wish to examine heat flow through material that is multidimensional. In those cases, u is a multivariable function of each dimension as well as time, and a single partial derivative won't do. Additionally, the quantity ϕ given for flux becomes a vector, and is therefore written as $\vec{\phi}$.

To rework the heat equation to reflect these changes, we must look back to the principle of heat energy conservation, expressed mathematically by (1.3.5). The 1-D partial derivative on the right-hand side is inadequate for ϕ , since we must give partial derivatives for all dimensions. Since the number of dimensions is generally arbitrary, we use the gradient operator ∇ and rewrite (1.3.5) as

$$\rho c \frac{\partial u}{\partial t} = \nabla \cdot \phi + Q \quad (1.3.10)$$

where (\cdot) is the dot product operator. Note that we are going to assume early that our material is uniform and thus ρ and c are constant. With no extra sources of heat (as before), we also have $Q = 0$.

In multiple dimensions we also must take a second look at Fourier's law of conductivity. With u being multidimensional, the single partial derivative seen in (1.3.6) is again inadequate. We replace it with the gradient operator ∇ and get

$$\phi = -K_0 \nabla u \quad (1.3.11)$$

which verifies our earlier assertion that ϕ is vector-valued. Note that K_0 is again constant.

Substituting (1.3.11) into (1.3.10) gives

$$\rho c \frac{\partial u}{\partial t} = K_0 \nabla \cdot (\nabla u). \quad (1.3.12)$$

By dividing by ρc and substituting κ as before, we are then left with

$$\frac{\partial u}{\partial t} = \kappa \nabla^2 u \quad (1.3.13)$$

as our multidimensional equation, where ∇^2 is the Laplacian operator.¹

1.3.3 Examining Convection

When the material being considered is stationary, then the heat equation given by (1.3.13) is satisfactory. When the material is more fluid and is itself flowing, however, we must examine how heat flows through the material in motion, a process known as convection. Suppose, then, that the fluid is moving with average velocity \mathbf{V} (not necessarily constant). Then the flux vector for the material changes to reflect this new property and takes on a term to account for the motion of the material affecting the flow of heat energy. Fourier's law of conductivity is then rewritten as

$$\phi = -K_0 \nabla u + \rho c u \mathbf{V}. \quad (1.3.14)$$

As usual, we substitute (1.3.14) into the equation for conservation of heat energy to arrive at our desired heat equation. Assuming again that $Q = 0$ and

¹The Laplacian can alternatively be designated by a Δ operator.

the material is uniform (i.e., ρ , c , and K_0 are constant), we get

$$\begin{aligned}
\rho c \frac{\partial u}{\partial t} &= -\nabla \cdot \phi = -\nabla \cdot (-K_0 \nabla u + \rho c u \mathbf{V}) \\
&\Rightarrow \rho c \frac{\partial u}{\partial t} = \nabla \cdot (K_0 \nabla u) - \nabla \cdot (\rho c u \mathbf{V}) \\
&\Rightarrow \rho c \frac{\partial u}{\partial t} = K_0 \nabla^2 u - \rho c \nabla \cdot (u \mathbf{V}) \\
&\Rightarrow \frac{\partial u}{\partial t} = \kappa \nabla^2 u - \mathbf{V} \cdot \nabla u - u \nabla \cdot \mathbf{V} \\
&\Rightarrow \frac{\partial u}{\partial t} + \mathbf{V} \cdot \nabla u = \kappa \nabla^2 u - u \nabla \cdot \mathbf{V}
\end{aligned}$$

where $\kappa = \frac{K_0}{\rho c}$, as before. In many cases, the velocity of the fluid is constant, and so

$$\nabla \cdot \mathbf{V} = 0.$$

This gives us a heat equation that accounts for convection of

$$\frac{\partial u}{\partial t} + \mathbf{V} \cdot \nabla u = \kappa \nabla^2 u. \quad (1.3.15)$$

1.4 Sturm-Liouville Theory

As we delve further into our problem with the heat equation, we will encounter a special class of differential equations (in particular, boundary-value problems) known as Sturm-Liouville problems (named for mathematicians Charles-François Sturm and Joseph Liouville) which have a special set of properties and identities.

1.4.1 Definitions and Lagrange's Identity

In general, Sturm-Liouville problems have the following form:

$$[p(x)y']' - q(x)y + \lambda r(x)y = 0 \quad (1.4.1)$$

$$a_1 y(0) + a_2 y'(0) = 0 \quad (1.4.2)$$

$$b_1 y(1) + b_2 y'(1) = 0 \quad (1.4.3)$$

where $0 < x < 1$. It is generally assumed that p , p' , q , and r are all continuous on $0 \leq x \leq 1$, and that $p(x) > 0$ and $r(x) > 0$ on the same interval. An alternate way of expressing (1.4.1) is by introducing the linear operator $L[y]$ as

$$L[y] = -[p(x)y']' + q(x)y \quad (1.4.4)$$

and then rewrite the differential equation as

$$L[y] = \lambda r(x)y. \quad (1.4.5)$$

The linear operator defined by (1.4.4) is useful in a number of ways. If we assume the functions $u(x)$ and $v(x)$ satisfy the boundary-value problem defined by (1.4.1), then the operator allows us to compute

$$\int_0^1 L[u]v dx = \int_0^1 -(pu')'v + quv dx. \quad (1.4.6)$$

Integration by parts of the first term on the right-hand side gives us

$$\int_0^1 -(pu')'v + quv dx = -pu'v \Big|_0^1 - \int_0^1 pu'v' + quv dx \quad (1.4.7)$$

$$= -pu'v \Big|_0^1 - \left[pu'v' \Big|_0^1 - \int_0^1 (pv')'u + quv dx \right] \quad (1.4.8)$$

$$= -p(u'v - uv') \Big|_0^1 + \int_0^1 L[v]u dx. \quad (1.4.9)$$

If we rearrange the terms in the equality of the left-hand side of (1.4.6) and (1.4.9), then we can produce the equation

$$\int_0^1 L[u(x)]v(x) - L[v(x)]u(x) dx = -p(x) [u(x)'v(x) - u(x)v'(x)] \Big|_0^1 \quad (1.4.10)$$

which is known as Lagrange's identity. Furthermore, if we also assume that $u(x)$ and $v(x)$ also satisfy the boundary conditions given by (1.4.2)-(1.4.3), then it can be shown that (1.4.10) becomes

$$\int_0^1 L[u(x)]v(x) - L[v(x)]u(x) dx = 0 \quad (1.4.11)$$

provided $a_2 \neq 0$ and $b_2 \neq 0$. It is useful, now, if we define an inner product for two functions that satisfy a Sturm-Liouville problem. To that end, using our familiar u and v , we define the following:

$$(u, v) = \int_0^1 u(x)v(x) dx \quad (1.4.12)$$

which allows us to rewrite (1.4.11) as

$$(L[u], v) - (u, L[v]) = 0. \quad (1.4.13)$$

Note that the inner product (1.4.12) is valid if both u and v are real-valued functions. If they are complex functions, then the inner product takes the form

$$(u, v) = \int_0^1 u(x)\overline{v(x)} dx \quad (1.4.14)$$

where $\overline{v(x)}$ is the complex-conjugate of $v(x)$. Note that even if u and v are real-valued, then (1.4.14) remains valid since $\overline{v(x)} = v(x)$ for real v .

1.4.2 Eigenvalues and Eigenfunctions

In (1.4.1), the constant λ represents an eigenvalue of the differential equation. We now investigate several properties of a Sturm-Liouville problem's eigenvalues by way of a few theorems.

Theorem 1.4.1. All eigenvalues of the Sturm-Liouville problem given by (1.4.1)-(1.4.3) are real.

Proof. Suppose λ is a nonzero eigenvalue corresponding to a nonzero eigenfunction $\phi(x)$. For this proof, we will allow for the possibility that λ and ϕ may both be complex. To the end, we define the two as follows:

$$\lambda := \mu + i\nu \quad \text{and} \quad \phi(x) := U(x) + iV(x) \quad (1.4.15)$$

where μ , ν , U , and V are all real. In the identity (1.4.13), allow both $u = \phi$ and $v = \phi$. This gives us

$$(L[\phi], \phi) - (\phi, L[\phi]) = 0 \Rightarrow (L[\phi], \phi) = (\phi, L[\phi]).$$

Using the identities given in (1.4.4) and (1.4.12), we have

$$\begin{aligned} (L[\phi], \phi) = (\phi, L[\phi]) &\Rightarrow (\lambda r\phi, \phi) = (\phi, \lambda r\phi) \\ &\Rightarrow \int_0^1 \lambda r\phi\bar{\phi} dx = \int_0^1 \phi\overline{\lambda r\phi} dx. \end{aligned}$$

Since $r(x)$ is a real-valued function, we have $\bar{r} = r$. From there, we have

$$\lambda \int_0^1 r\phi\bar{\phi} dx - \bar{\lambda} \int_0^1 r\bar{\phi}\phi dx = (\lambda - \bar{\lambda}) \int_0^1 r\phi\bar{\phi} dx = 0.$$

Using the definition of ϕ given in (1.4.15), we find that

$$\phi\bar{\phi} = |\phi|^2 = U(x)^2 + V(x)^2$$

and so

$$(\lambda - \bar{\lambda}) \int_0^1 r(x) [U(x)^2 + V(x)^2] dx = 0. \quad (1.4.16)$$

Since $r(x)$ and $\phi(x)$ are both nonzero, then the integrand in (1.4.16) cannot be zero. We are therefore left with

$$\lambda - \bar{\lambda} = 0 \Rightarrow 2i\nu = 0 \Rightarrow \nu = 0.$$

Therefore, λ must be real. □

As a result of this theorem, solving Sturm-Liouville problems is made simpler because we are spared the task of seeking complex eigenvalues. It can also be shown that the eigenfunctions of Sturm-Liouville problems are also strictly real-valued.

This next theorem establishes the principle of orthogonality for the eigenfunctions of Sturm-Liouville problems.

Theorem 1.4.2. If $\phi_1(x)$ and $\phi_2(x)$ are two eigenfunctions of the Sturm-Liouville problem given by (1.4.1)-(1.4.3) that correspond to *distinct* eigenvalues λ_1 and λ_2 , respectively, then

$$\int_0^1 r(x)\phi_1(x)\phi_2(x) dx = 0.$$

Proof. From (1.4.4), we know that

$$L[\phi_1] = \lambda_1 r\phi_1 \quad \text{and} \quad L[\phi_2] = \lambda_2 r\phi_2. \quad (1.4.17)$$

Referring back to (1.4.12), if we allow $u = \phi_1$ and $v = \phi_2$, we have

$$\begin{aligned} (L[\phi_1], \phi_2) - (\phi_1, L[\phi_2]) &= 0 \Rightarrow (\lambda_1 r\phi_1, \phi_2) - (\phi_1, \lambda_2 r\phi_2) = 0 \\ &\Rightarrow \lambda_1 \int_0^1 r(x)\phi_1(x)\phi_2(x) dx - \lambda_2 \int_0^1 \phi_1(x)r(x)\phi_2(x) dx = 0 \\ &\Rightarrow (\lambda_1 - \lambda_2) \int_0^1 r(x)\phi_1(x)\phi_2(x) dx = 0. \end{aligned}$$

Since λ_1 and λ_2 are distinct, then $\lambda_1 - \lambda_2 \neq 0$, and so

$$\int_0^1 r(x)\phi_1(x)\phi_2(x) dx = 0. \quad \square$$

The preceding theorem depended on the two eigenvalues being distinct with respect to the two different eigenfunctions. In the following lemma, we will establish that each eigenvalue of a Sturm-Liouville problem corresponds uniquely to a certain eigenfunction.

Lemma. *The eigenvalues of the Sturm-Liouville problem given by (1.4.1)-(1.4.3) are simple; or, each eigenvalue corresponds to one linearly independent eigenfunction.*

Proof. Suppose λ is an eigenvalue corresponding to two different linearly independent eigenfunctions ϕ_1 and ϕ_2 . If we compute the Wronskian of ϕ_1 and ϕ_2 , we have

$$W(\phi_1, \phi_2)(x) = \begin{vmatrix} \phi_1(x) & \phi_2(x) \\ \phi_1'(x) & \phi_2'(x) \end{vmatrix} = \phi_1(x)\phi_2'(x) - \phi_1'(x)\phi_2(x) \quad (1.4.18)$$

By definition, ϕ_1 and ϕ_2 are linearly independent if and only if the Wronskian $W(\phi_1, \phi_2)(x)$ is never 0. At the point $x = 0$, however, we have the following:

$$\begin{aligned} W(\phi_1, \phi_2)(0) &= \phi_1(0)\phi_2'(0) - \phi_1'(0)\phi_2(0) \\ &= \phi_1(0) \left(-\frac{a_1}{a_2} \phi_2(0) \right) - \left(-\frac{a_1}{a_2} \phi_1(0) \right) \phi_2(0) \\ &= -\frac{a_1}{a_2} \phi_1(0)\phi_2(0) + \frac{a_1}{a_2} \phi_1(0)\phi_2(0) \\ &= 0 \end{aligned}$$

using both (1.4.2) and the assumption that $a_2 \neq 0$. Since the Wronskian is 0 at some point, then ϕ_1 and ϕ_2 are not linearly independent, and we arrive at a contradiction to the premise at the beginning of the proof. Therefore, the eigenvalues of a Sturm-Liouville problem are simple. \square

1.4.3 Singular Sturm-Liouville Problems

With the Sturm-Liouville problems we have worked with so far, we have always assumed regularity. In other words, we have always assumed that the properties associated with p , q , etc. have all held true throughout the problem. But in some physical phenomena, one or more of these properties doesn't hold, and typically this occurs on a boundary (i.e. at $x = 0$ or $x = 1$). For the differential equations that are almost of the Sturm-Liouville variety, we classify them as singular Sturm-Liouville problems. These kinds of problems have all the same properties as regular Sturm-Liouville problems on the open interval $0 < x < 1$, but at least one property fails at either one or both boundaries. Singular Sturm-Liouville problems can also refer to differential equations defined on an open interval (e.g. $0 < x < \infty$).

Consider the following differential equation

$$xy'' + y' + \lambda xy = 0 \quad \text{or} \quad -(xy')' = \lambda xy \quad (1.4.19)$$

with boundary conditions

$$y(0) = 0 \quad (1.4.20)$$

$$y(1) = 1 \quad (1.4.21)$$

defined on the interval $0 < x < 1$ with $\lambda > 0$. Notice that the criteria for being a Sturm-Liouville problem appear to all be met, except for one. The coefficient $r(x) = x$ must be positive over the closed interval (i.e. $0 \leq x \leq 1$, yet we have $r(0) = 0$). Therefore, we can classify this boundary-value problem as a singular Sturm-Liouville problem. To solve this problem, we can begin to proceed as we would for any other problem, but we will have to deal with the singularity at $x = 0$ eventually. For now, though, we apply elementary methods.

Making the substitution $t = \sqrt{\lambda}x$, we have $y'(x) = \sqrt{\lambda}y'(t)$ and $y''(x) = \lambda y''(t)$ by the chain rule. Making those substitutions into (1.4.19) gives us

$$t \frac{\lambda}{\sqrt{\lambda}} y'' + \sqrt{\lambda} y' + t \frac{\lambda}{\sqrt{\lambda}} y = 0$$

which simplifies to

$$ty'' + y' + ty = 0. \quad (1.4.22)$$

The differential equation (1.4.22) is easily identifiable as Bessel's equation of order 0. The solution in t is given by

$$y(t) = c_1 J_0(t) + c_2 Y_0(t)$$

with a general solution in x of

$$y(x) = c_1 J_0(\sqrt{\lambda}x) + c_2 Y_0(\sqrt{\lambda}x). \quad (1.4.23)$$

where c_1 and c_2 are arbitrary constants and J_0 and Y_0 represent zero-order Bessel functions of the first and second time, respectively. The explicit definitions for J_0 and Y_0 are very intricate, and are therefore omitted. Turning our attention now to the boundary conditions given by (1.4.20)-(1.4.21), we see that $J_0(0) = 1$, yet $Y_0(x) \rightarrow -\infty$ as $x \rightarrow 0$. Because of this, we must choose $c_1 = 0$ and $c_2 = 0$ (the trivial solution) so that (1.4.23) can satisfy the boundary conditions.

Obviously, the trivial solution isn't satisfactory, so we need to find a workaround so that $y(x)$ can be non-trivial. One common method is to change one or both boundary conditions to one that is less restrictive. In this case, we will modify (1.4.20), since that is the one which was problematic before. Rather than require $y(0) = 0$, we will instead require that y and y' be bounded as $x \rightarrow 0$.

Since both Y_0 and Y_0' are unbounded as $x \rightarrow 0$, then we set $c_2 = 0$. This leaves us with

$$y(x) = c_1 J_0(\sqrt{\lambda}x). \quad (1.4.24)$$

Our second boundary condition, given by (1.4.21), gives us

$$y(1) = c_1 J_0(\sqrt{\lambda}) = 0$$

which can be shown to have an infinite series of positive roots $0 < \lambda_1 < \lambda_2 < \lambda_3 < \dots$, giving us a set of eigenvalues. The corresponding eigenfunctions are given by

$$\phi_n(x) = J_0(\sqrt{\lambda_n}x).$$

The constants c will be computed in the next section.

This example is intended to illustrate how to take a singular Sturm-Liouville problem can be solved by relaxing certain boundary conditions to the point where intuitive eigenvalues and eigenfunctions can be computed. The use of this process, however, leaves open two important questions concerning singular Sturm-Liouville problems:

1. What kind of boundary conditions can be allowed in a singular Sturm-Liouville problem?
2. How closely do the properties of the eigenvalues and eigenfunctions of a singular Sturm-Liouville problem mirror those of a regular Sturm-Liouville problem? For example, are the eigenvalues real and are the eigenfunctions orthogonal?

The answers to these questions depend on the identity

$$\int_0^1 L[u]v - L[v]u \, dx = 0$$

and under what conditions it holds true for singular Sturm-Liouville problems.[1]

1.4.4 Method of Eigenfunction Expansion

In the example in the previous section, we outlined how to solve a singular Sturm-Liouville problem, but we didn't quite finish, since we left the constants c arbitrary. To compute them numerically, we use a method known as eigenfunction expansion.[3]

We begin by recalling Theorem 1.4.2, which said that the eigenfunctions of a Sturm-Liouville problem are orthogonal. While this problem was singular, it can be shown that this orthogonality extends to Bessel functions as well. Therefore, our eigenfunctions given by (1.4.24) have the property

$$\int_0^1 r(x)\phi_m(x)\phi_n(x) dx = \int_0^1 x\phi_m(x)\phi_n(x) dx = 0$$

when $m \neq n$. Using the superposition principle, we have that

$$y(x) = \sum_{n=1}^{\infty} c_n \phi_n(x) = \sum_{n=1}^{\infty} c_n J_0(\sqrt{\lambda_n}x). \quad (1.4.25)$$

Multiplying both sides of (1.4.25) by $xJ_0(\sqrt{\lambda_m}x)$ and integrating with respect to x from 0 to 1 gives

$$\int_0^1 xy(x)J_0(\sqrt{\lambda_m}x) dx = \sum_{n=1}^{\infty} c_n \int_0^1 xJ_0(\sqrt{\lambda_m}x)J_0(\sqrt{\lambda_n}x) dx$$

which, because of orthogonality, quickly reduces to

$$\int_0^1 xy(x)J_0(\sqrt{\lambda_m}x) dx = c_m \int_0^1 xJ_0^2(\sqrt{\lambda_m}x) dx.$$

Therefore, we have

$$c_m = \frac{\int_0^1 xy(x)J_0(\sqrt{\lambda_m}x) dx}{\int_0^1 xJ_0^2(\sqrt{\lambda_m}x) dx}. \quad (1.4.26)$$

Chapter 2

Boundary Value Problem Derivation and Solution

2.1 Problem Development

In this model, we examine the temperature of the fluid in a single stage of the pipe, where the pipe's width is uniform throughout the section. We will solve the steady-state of the problem (i.e. assume $\partial T/\partial t = 0$) and assume the liquid has Hagen-Poiseuille flow. Additionally, while we consider that the geothermal properties of the soil surrounding the pipe has an effect on the liquid's temperature profile, we will assume that the converse does not apply. To this end, we assume that the temperature profile of the liquid along the edge of the pipe matches that of the surrounding soil. This model will be constructed in a Cartesian coordinate system with axes defined by the centerline of the pipe and its base ($x = 0$ and $z = 0$, respectively). We will assume symmetry about the x -axis.

The pipe under consideration has the following physical properties:

Property	Representative variable	Typical numerical value
Width	R^*	5 cm
Length	L^*	1 km
Flow velocity	W^*	32 L/s (.032 m/s)

Table 2.1.1: Physical properties of the pipe

To construct the model, we begin with the equation for heat energy of fluid flow in vector form:

$$\rho c_p \left(\frac{\partial T}{\partial t} + \mathbf{u} \cdot \nabla T \right) = k \nabla^2 T \quad (2.1.1)$$

where

$$\mathbf{u} = u \hat{\mathbf{x}} + w \hat{\mathbf{z}} \quad (2.1.2)$$

with $\hat{\mathbf{x}}$ and $\hat{\mathbf{z}}$ being unit vectors. The following table describes other variables and coefficients in (2.1.1) as well as other variables and coefficients to be introduced in this section:

Variable	Description
ρ	Density of the fluid in the pipe
c_p	The fluid's specific heat capacity
k	The fluid's conductivity constant
h	Heat transfer coefficient
T_g	Thermal profile of the soil around the pipe
κ	The fluid's thermal diffusivity

Table 2.1.2: Variables and coefficients in (2.1.1), etc.

This equation represents the conservation of energy of the fluid in the pipe.

The definition in (2.1.2) allows us to expand the gradient in (2.1.1). With this, and applying the steady-state assumption, (2.1.1) becomes

$$\rho c_p \left(\frac{\partial T}{\partial t} + uT_x + wT_z \right) = k \nabla^2 T. \quad (2.1.3)$$

Because we have assumed that the temperature profile of the liquid has no measurable effect on the soil around the pipe when in fact the converse is true, we have a Robin boundary condition of

$$kT_x = -h(T - T_g). \quad (2.1.4)$$

Within h , we assume that the liquid's flow is turbulent, and that there is a Dittus-Boelter correlation with a Reynolds number $Re = 10^5$ and a relatively small Prandtl number (for water, this number is 7) which makes h large.

2.1.1 Nondimensionalization

Before proceeding further, we can nondimensionalize a number of variables for with the substitutions

$$\begin{aligned} x &\Rightarrow R \\ z &\Rightarrow L \\ w &\Rightarrow W \\ u &\Rightarrow \frac{R}{L}W \\ t &\Rightarrow \frac{L}{W} \\ \Theta &\Rightarrow \frac{1}{T_{AMB}}(T - T_{AMB}) \end{aligned}$$

where $R, W, L \in [0, 1]$ and T_{AMB} is the temperature at top of the pipe. We then make the appropriate substitutions into (2.1.3) to get

$$\rho c_p \left(\frac{RW}{L} \Theta_x + \frac{W}{L} \Theta_z w \right) = k \left(\Theta_{xx} + \frac{R^2}{L^2} \Theta_{zz} \right) \quad (2.1.5)$$

Factoring and applying the substitutions $\epsilon = \frac{R}{L}$ and $\kappa = \frac{k}{\rho c_p}$ makes the equation

$$\epsilon \left(\frac{WR}{\kappa} \right) (u \Theta_x + w \Theta_z) = \Theta_{xx} + \epsilon^2 \Theta_{zz} \quad (2.1.6)$$

With Hagen-Poiseuille flow in the model, we apply the conditions

$$u = u(x) = 0$$

and

$$w = w(x) = \frac{(R^*)^2 - x^2}{(R^*)^4}$$

Applying these substitutions to (2.1.6) makes it

$$\epsilon \text{Pe} w(x) \Theta_z = \Theta_{xx} + \epsilon^2 \Theta_{zz} \quad (2.1.7)$$

where $\text{Pe} = \frac{WR}{\kappa}$. The following table describes the coefficients in (2.1.7):

Coefficient	Description
ϵ	Ratio of pipe's width to its length (dimensionless)
Pe	Péclet number (dimensionless)

Table 2.1.3: Coefficients in (2.1.7)

If we examine ϵ , we notice that it divides the width of the well (on the order of a few centimeters) by the well's length (on the order of a few kilometers), which not only makes ϵ very small, but also makes ϵ^2 small to the point that we can allow

$$\epsilon^2 \rightarrow 0.$$

Notice also that the Péclet number is relatively large. Rather than dealing with multiplying a large number by a much smaller one, we can define a new constant as

$$\overline{\text{Pe}} = \epsilon \text{Pe}$$

instead. If we apply both of these to (2.1.7), we arrive at the nondimensional equation

$$\overline{\text{Pe}} w(x) \Theta_z = \Theta_{xx}, \quad x \in [0, R^*], \quad z \in [0, L^*] \quad (2.1.8)$$

with boundary conditions

$$\Theta_x(0, z) = 0 \quad (2.1.9)$$

$$\Theta(R^*, z) = \Theta_g(z) \quad (2.1.10)$$

$$\Theta(x, 0) = \Theta_g(0). \quad (2.1.11)$$

This can be solved using separation of variables.

2.1.2 Separation of Variables

To begin solving the BVP (2.1.8)-(2.1.11) using separation of variables, we first define $\Theta(x, z)$ as a product of two single-variable functions $\phi(x)$ and $Z(z)$, i.e.

$$\Theta(x, z) = \phi(x)Z(z). \quad (2.1.12)$$

From (2.1.12), we can see that

$$\Theta_z = \phi(x)Z'(z) \quad \text{and} \quad \Theta_{xx} = \phi''(x)Z(z).$$

This turns (2.1.8) into

$$\overline{\text{Pe}}w(x)\phi(x)Z'(z) = \phi''(x)Z(z). \quad (2.1.13)$$

To separate the variables, we divide both sides of (2.1.13) by $w(x)\phi Z$ so that each side of the equation is expressed in terms of only one variable, giving us

$$\frac{\overline{\text{Pe}}Z'(z)}{Z(z)} = \frac{\phi''(x)}{w(x)\phi(x)}. \quad (2.1.14)$$

We now note that since both sides of (2.1.14) are expressed in terms of different variables, then the equality allows us to define each side as the same constant. We therefore define

$$\frac{\overline{\text{Pe}}Z'(z)}{Z(z)} = \frac{\phi''(x)}{w(x)\phi(x)} = -\lambda$$

which can be separated into the system

$$\overline{\text{Pe}}Z' + \lambda Z = 0 \quad (2.1.15)$$

$$\phi'' + \lambda w(x)\phi = 0 \quad (2.1.16)$$

giving us an eigenvalue problem in x and an amplitude problem in z .

Before we solve (2.1.16), we first scale x and introduce the variable

$$\xi = \frac{x}{R^*}$$

which has a range of $[0, 1]$. This turns $w(x)$ into

$$\begin{aligned} w(\xi) &= \frac{(R^*)^2 - \xi^2(R^*)^2}{(R^*)^4} \\ &= \frac{1 - \xi^2}{(R^*)^2}. \end{aligned}$$

Additionally, the chain rule tells us that

$$\phi''(\xi) = \frac{d^2\phi}{d\xi^2} = \frac{d^2\phi}{dx^2} \left(\frac{dx}{d\xi}\right)^2 + \frac{d\phi}{dx} \frac{d^2x}{d\xi^2} = \phi''(x)(R^*)^2 \Rightarrow \phi''(x) = \frac{\phi''(\xi)}{(R^*)^2}$$

where we see that $(R^*)^2$ is a common denominator that can be cancelled. Therefore, the eigenvalue problem we are faced with is

$$\phi''(\xi) + \lambda(1 - \xi^2)\phi(\xi) = 0 \tag{2.1.17}$$

with boundary conditions

$$\phi'(0) = 0 \tag{2.1.18}$$

$$\phi(1) = 0. \tag{2.1.19}$$

2.2 Finding the Basis Eigenfunctions

We are faced with the task of finding the eigenvalues and eigenfunctions of the following BVP:

$$\phi''(\xi) + \lambda(1 - \xi^2)\phi(\xi) = 0 \tag{2.2.1}$$

$$\phi'(0) = 0 \tag{2.2.2}$$

$$\phi(1) = 0. \tag{2.2.3}$$

We can quickly recognize this problem as a Sturm-Liouville problem, and so we can derive the eigenfunctions from an orthogonal basis function ψ that solves

$$\psi''(\xi) + \mu\psi(\xi) = 0 \tag{2.2.4}$$

$$\psi'(0) = 0 \tag{2.2.5}$$

$$\psi(1) = 0 \tag{2.2.6}$$

2.2.1 Finding the Basis Functions ϕ

The boundary value problem given by (2.2.4)-(2.2.6) has a general solution of

$$\psi(\xi) = c_1 \cos(\sqrt{\mu}\xi) + c_2 \sin(\sqrt{\mu}\xi) \tag{2.2.7}$$

where c_1 and c_2 are arbitrary constants. To apply (2.2.5), we first compute

$$\psi'(\xi) = -\sqrt{\mu}c_1 \sin(\sqrt{\mu}\xi) + \sqrt{\mu}c_2 \cos(\sqrt{\mu}\xi)$$

and then find

$$\psi'(0) = \sqrt{\mu}c_2 = 0 \Rightarrow c_2 = 0 \tag{2.2.8}$$

because we assume $\mu > 0$. Applying (2.2.6) gives

$$\psi(1) = c_1 \cos(\sqrt{\mu}) = 0. \tag{2.2.9}$$

To avoid a trivial solution (i.e. $c_1 = 0$), we consider $\cos(\sqrt{\mu}) = 0$, which gives us eigenvalues of

$$\mu_i = \frac{\pi^2}{4} (2i - 1)^2 \quad (2.2.10)$$

where $i \in \mathbb{Z}$. Thus, our basis function is given by

$$\psi_i(\xi) = \cos(\sqrt{\mu_i}\xi). \quad (2.2.11)$$

To compute $\phi(\xi)$ from the basis $\psi(\xi)$, we apply the superposition principle to give us

$$\phi(\xi) = \sum_{i=1}^{\infty} c_i \psi_i(\xi). \quad (2.2.12)$$

2.2.2 Using Eigenfunction Expansion to Find Eigenvectors

To compute the constants c_i , we multiply both sides of (2.2.12) by $\psi_j(\xi)$ and integrate from 0 to 1 with respect to ξ . This gives us

$$\int_0^1 \phi(\xi) \psi_j(\xi) d\xi = \sum_{i=1}^{\infty} c_i \int_0^1 \psi_i(\xi) \psi_j(\xi) d\xi. \quad (2.2.13)$$

Because of the orthogonality relation of the cosine function with itself, we can reduce the right-hand side of (2.2.13) and rewrite it as

$$\int_0^1 \phi(\xi) \psi_j(\xi) d\xi = c_j \int_0^1 \psi_j^2(\xi) d\xi \quad (2.2.14)$$

which gives us the following formula for c_i :

$$c_i = \frac{\int_0^1 \phi(\xi) \psi_i(\xi) d\xi}{\int_0^1 \psi_i^2(\xi) d\xi}. \quad (2.2.15)$$

With (2.2.15), we can proceed with finding the eigenvalue λ from (2.2.1).

2.2.3 Numerically Computing the Eigenvectors

Multiplying (2.2.15) by $\psi_j(\xi)$ and then integrating from 0 to 1 with respect to ξ gives us the following integral equation:

$$\int_0^1 \psi_j(\xi) \phi''(\xi) d\xi + \int_0^1 \lambda (1 - \xi^2) \phi(\xi) \psi_j(\xi) d\xi = 0. \quad (2.2.16)$$

From (2.2.12), we can rewrite the second term of (2.2.16) as

$$\sum_{i=1}^{\infty} c_i \int_0^1 \lambda (1 - \xi^2) \psi_i(\xi) \psi_j(\xi) d\xi. \quad (2.2.17)$$

The first term, on the other hand, can be rewritten using integration by parts:

$$\begin{aligned}\int_0^1 \psi_j(\xi)\phi''(\xi)d\xi &= \psi_j(\xi)\phi'(\xi)\Big|_0^1 - \int_0^1 \psi_j'(\xi)\phi'(\xi)d\xi \\ &= -\left[\psi_j'(\xi)\phi(\xi)\Big|_0^1 - \int_0^1 \psi_j''(\xi)\phi(\xi)d\xi\right] \\ &= \int_0^1 \psi_j''(\xi)\phi(\xi)d\xi.\end{aligned}$$

Using (2.2.4) and (2.2.15), the last integral can be rewritten as

$$\begin{aligned}\int_0^1 \psi_j''(\xi)\phi(\xi)d\xi &= -\mu_j \int_0^1 \psi_j(\xi)\phi(\xi)d\xi \\ &= -\mu_j \int_0^1 \psi_j^2(\xi)d\xi \\ &= -\frac{1}{2}\mu_j c_j\end{aligned}\tag{2.2.18}$$

Now, with (2.2.17) and (2.2.18), we see that (2.2.16) is equivalent to

$$-\frac{1}{2}\mu_j c_j + \sum_{i=1}^{\infty} c_i \int_0^1 \lambda(1-\xi^2)\psi_i(\xi)\psi_j(\xi)d\xi = 0\tag{2.2.19}$$

which establishes a relation between the eigenvalues λ and the coefficients c . For computational purposes, we can restrict our sum in (2.2.19) to the first N terms. Doing so allows us to write (2.2.19) as an algebraic equation with the form

$$\frac{1}{2}M\mathbf{c} = \lambda B\mathbf{c}\tag{2.2.20}$$

where M is a diagonal matrix of the eigenvalues $\mu_1, \mu_2, \dots, \mu_N$, \mathbf{c} is a column vector of the coefficients c_1, c_2, \dots, c_N , and B is a matrix with

$$\int_0^1 (1-\xi^2)\cos(\sqrt{\mu_i}\xi)\cos(\sqrt{\mu_j}\xi)d\xi\tag{2.2.21}$$

as its ij -th element.

2.3 Solving for the Nondimensional Θ

Now that we have computed our eigenfunctions $\phi_i(\xi)$, we can turn our attention back to the nondimensional boundary-value problem in $\Theta(\xi, z)$ given in part by

$$\overline{\text{Pe}}(1-\xi^2)\Theta_z = \Theta_{\xi\xi}\tag{2.3.1}$$

$$\Theta(\xi, 0) = \Theta_g(0)\tag{2.3.2}$$

where $\overline{\text{Pe}}$ is the product of the Péclet number and ϵ given before. We first note that we are still working in the context of a Sturm-Liouville problem, and that our eigenfunctions have an orthonormal relationship given by

$$\int_0^1 \phi_i(\xi)\phi_j(\xi)(1-\xi^2)d\xi = \begin{cases} 0 & \text{if } i \neq j \\ 1 & \text{if } i = j \end{cases} \quad (2.3.3)$$

by Theorem 1.4.2. Recall also that $\phi_i(\xi)$ is only one half of $\Theta(\xi, z)$ and that the other half, $Z(z)$, must also be computed. Bringing them together gives us

$$\Theta_i(\xi, z) = \phi_i(\xi)Z_i(z). \quad (2.3.4)$$

With the superposition principle, we can then set Θ to

$$\Theta(\xi, z) = \sum_{i=1}^{\infty} \phi_i(\xi)Z_i(z). \quad (2.3.5)$$

To compute $Z(z)$, we first multiply (2.3.5) by $\phi_j(\xi)(1-\xi^2)$ and then integrate with respect to ξ from 0 to 1, which gives us

$$\int_0^1 \Theta(\xi, z)\phi_j(\xi)(1-\xi^2)d\xi = \sum_{i=1}^{\infty} \int_0^1 \phi_i(\xi)Z_i(z)\phi_j(\xi)(1-\xi^2)d\xi. \quad (2.3.6)$$

From the orthonormal relationship given in (2.3.3), we can reduce the right-hand side to just $Z_j(z)$, which gives us

$$Z_j(z) = \int_0^1 \Theta(\xi, z)\phi_j(\xi)(1-\xi^2)d\xi \quad (2.3.7)$$

with

$$Z_j(0) = \int_0^1 \Theta(\xi, 0)\phi_j(\xi)(1-\xi^2)d\xi = \int_0^1 \Theta_g(0)\phi_j(\xi)(1-\xi^2)d\xi. \quad (2.3.8)$$

To get a more explicit picture of $Z_j(z)$, we multiply (2.3.1) by $\phi_j(\xi)$ and integrate with respect to ξ from 0 to 1 to get

$$\int_0^1 \overline{\text{Pe}}(1-\xi^2)\Theta_z(\xi, z)\phi_j(\xi)d\xi = \int_0^1 \Theta_{\xi\xi}\phi_j(\xi)d\xi. \quad (2.3.9)$$

Applying (2.3.5) turns (2.3.9) into

$$\overline{\text{Pe}} \sum_{i=1}^{\infty} \int_0^1 (1-\xi^2)\phi_i(\xi)Z_i'(z)\phi_j(\xi)d\xi = \sum_{i=1}^{\infty} \int_0^1 \phi_i''(\xi)Z_i(z)\phi_j(\xi)d\xi. \quad (2.3.10)$$

Using (2.3.3) the left-hand side of (2.3.10) can be reduced to

$$\overline{\text{Pe}}Z_j'(z). \quad (2.3.11)$$

For the right-hand side, however, we must recall the boundary-value problem governing ϕ . Using that, we can rewrite the right-hand side as

$$-\sum_{i=1}^{\infty} \lambda_i \int_0^1 (1 - \xi^2) \phi_i(\xi) Z_i(z) \phi_j(\xi) d\xi \quad (2.3.12)$$

where λ_i is the eigenvalue corresponding to the i th eigenfunction. Applying (2.3.3) gives us

$$-\lambda_j Z_j(z). \quad (2.3.13)$$

Bringing (2.3.11) and (2.3.13), we can now rewrite (2.3.10) as

$$\overline{\text{Pe}} Z_j'(z) = -\lambda_j Z_j(z). \quad (2.3.14)$$

This ordinary differential equation in Z can easily be solved and has a general solution of

$$Z_j(z) = A \exp\left(-\frac{\lambda_j}{\overline{\text{Pe}}} z\right) \quad (2.3.15)$$

where A is an arbitrary constant. To compute A , we recall the initial condition given by (2.3.2) and compute

$$Z_j(0) = A \exp(0) \Rightarrow A = Z_j(0) \quad (2.3.16)$$

where $Z_j(0)$ is given explicitly above. We now have an explicit definition for $Z_i(z)$ and, consequently, $\Theta(\xi, z)$.

Chapter 3

Results

With the model constructed, various data were numerically computed and collected using Matlab. They gave insight into the temperature profile of the water in the Pullach well as well as where heat loss takes place. For all computations, an external profile $T_g = 1$ was used, but this can be easily changed and analyzed accordingly.

3.1 Temperature Rise in Each Mode

Each $\phi_i(\xi)$ represents a different mode, or section of the pipe. Each mode has its own width, and therefore its own temperature profile. The Matlab script `eigens.m` was used to numerically compute the temperature profile at various modes. Figure 3.1.1 shows the temperature profile of the first three modes. The values along the vertical axis show the temperature relative to the thermal profile of the edge of the well. Mathematically speaking, the temperature of the water in terms of the temperature along the edge of the well is given by

$$T_i(\xi) = (1 + \phi_i(\xi))T_g.$$

From the figure, we see that the profile of the first mode (the one at the bottom of the well), is the most stable, which isn't surprising since the temperature profile immediately below the well should match (or be reasonably close to) that of the edge of the bottom of the well. From there, the profiles get a bit more hectic. Moving away from the center of the pipe causes increased variation in the temperature of the water. Figure 3.1.2 shows the profiles of the fourth and fifth modes.

Consistent with the previous figure, the profiles get more hectic and vary more as you move further from the center of the pipe. This time, however, there appears to be some sort of consistency between the profiles. Indeed, as we plot higher modes, the shapes of the plots continue to look more similar to each other, although the numbers can vary quite a bit.

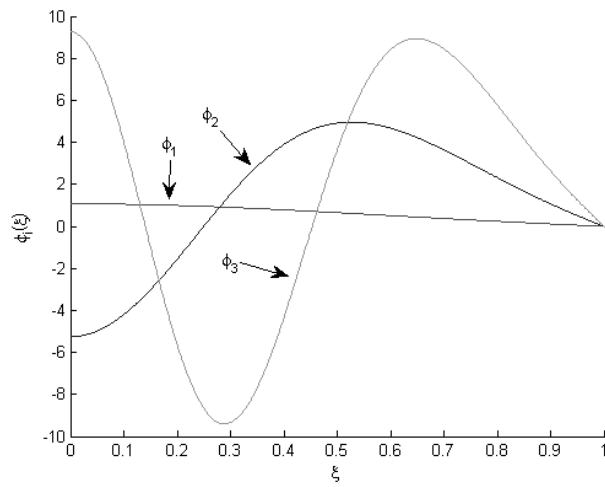


Figure 3.1.1: Temperature profiles of $\phi_1(\xi)$, $\phi_2(\xi)$, and $\phi_3(\xi)$.

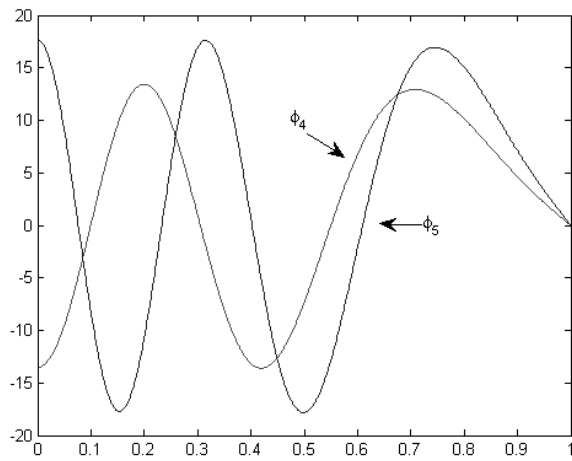


Figure 3.1.2: Temperature profiles of $\phi_4(\xi)$ and $\phi_5(\xi)$.

The Matlab function `nondim.m` computes values for the whole model, varying on the number of modes, the Péclet number, etc. With a low number of modes, we see similar results as with `eigens.m`: start with some stability and then quickly see less. But with high numbers of modes, the process of becoming more “hectic” slows down some, while the numbers do increase. Figure 3.1.3 illustrates this with a comparison of $N = 10$ (left) and $N = 5$ (right). Note the differences in the ranges of their vertical axes.

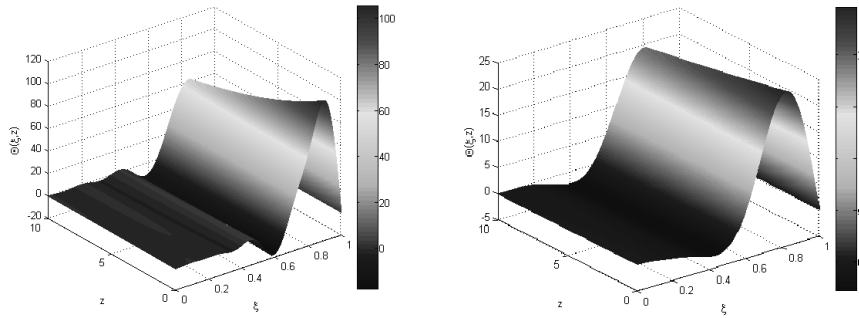


Figure 3.1.3: Full models for $N = 10$ (left) and $N = 5$ (right).

Notice also the shapes of the graphs as you move along the z -axis. Both are exponential, but the $N = 10$ model has a deeper slope to it, suggesting a higher drop in temperature. In fact, as N increases, so does this “depth”.

3.2 Variation of the Péclet Number

Recall that the Péclet number is directly proportional to the radius of the well (or, the radius of the current mode of the well) and inversely proportional to the thermal diffusivity of the water travelling in it. While the thermal diffusivity is more or less constant, the radius is something that can vary significantly. Thus, the Péclet number is itself a moving target. Exploring how the model changes based on the Péclet number yields some interesting results. Figure 3.1.3 above showed both $N = 10$ and $N = 5$ with a Péclet number of 1,000. Figure 3.2.1 below shows $N = 5$ with Péclet numbers of 100 and 500.

What is immediately noticeable is the difference in shape. As z increases, the model loses heat rather quickly for $\overline{Pe} = 100$, but this is not the case for neither $\overline{Pe} = 500$ nor $\overline{Pe} = 1000$. We see a similar result with the same Péclet numbers when $N = 10$, as illustrated by Figure 3.2.2.

It is also noteworthy that, in all the models and cases presented, heat tends to be highest when approaching $\xi = 1$, before tapering off to 0 (as prescribed by the boundary conditions).

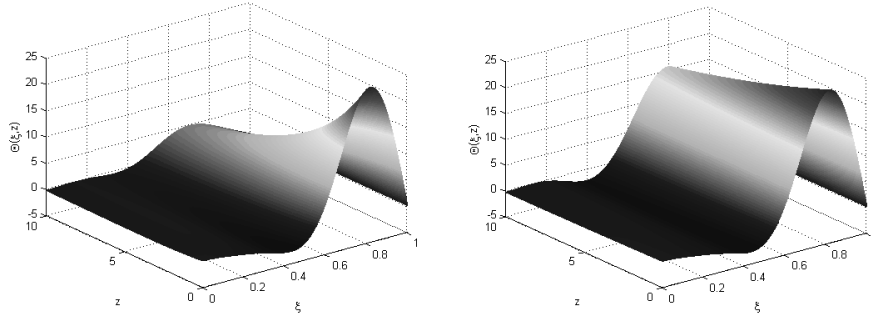


Figure 3.2.1: Model for $N = 5$ with $\overline{Pe} = 100$ (left) and $\overline{Pe} = 500$ (right).

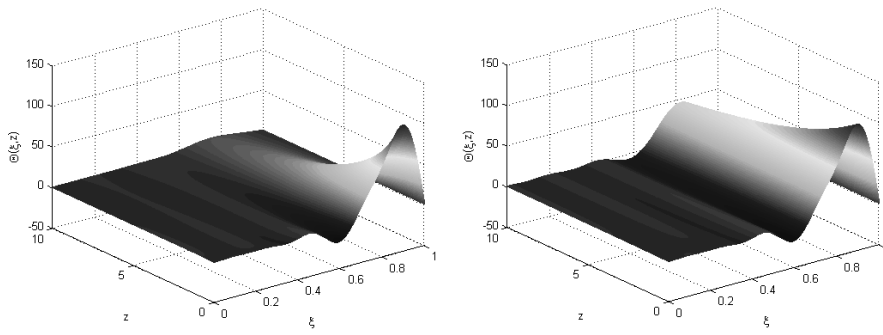


Figure 3.2.2: Model for $N = 10$ with $\overline{Pe} = 100$ (left) and $\overline{Pe} = 500$ (right).

Chapter 4

Conclusions

The data shown in the previous chapter is representative of all the data computed and collected throughout this project. Going back to the original problem, we now examine the physical applications of our results to the Pullach well.

4.1 Applying our Results

Clearly, heat is lost in the production well as the water makes its 5 km journey to the Earth's surface. After looking at the results, the decay of the heat appears to be exponential in nature, and so it would be expected that a deeper well would produce more lost heat. Consequently, the results could be similar if more modes were added. While initial temperature may be higher, the resulting heat loss could be greater. However, more research is needed to investigate whether there is causality here.

One notable result is that the water appears to become more heated as it nears the edge of the well before tapering off to match the temperature profile of the well's immediate surroundings. This is most likely a result of Fourier's law of conductivity which says, in part, that heat flows from hot to cold, with the center of the well being warmer than the earth around it. The buildup of heat near the edge is likely a result of the larger amount of water being near the edge as opposed to near the center.

The Péclet number carries a lot of influence in this model. If we are to interpret a relatively high Péclet number to indicate a relatively wide well, then we can conclude that a narrower well leads to more heat loss. This could again be a result of Fourier's law, as the heat energy doesn't have as far to travel before reaching its cold sink as it would in a wider well.

4.2 Future Work

Clearly, there is more to be done in this field. As mentioned previously, it should be looked into whether the number of modes in a well is a factor in how much

heat is lost. This could eventually lead to wells with uniform radius from top to bottom, or to wells more resembling cones in the future, or something in between. Also, more attention must be paid to the geothermal profile of the earth around the well, and how it and the water can influence each other (as opposed to just the earth influencing the water).

It could very well be that heat loss can be attributed to water seeping out of the well while it flows to the surface. Therefore, more research into the materials going into the wells is necessary. This research can investigate materials' porousness as well as their ability to seal heat within the well.

Finally, the Péclet number showed itself to be an important factor in this model. While the radius of the well is a significant part of it, the velocity of the water flow is also significant. Research could therefore be done as to whether artificially speeding up or slowing down water flow has any effect on temperature and heat loss. In addition, due to the impure nature of the water being extracted, more precise measurements of the water's thermal diffusivity would yield more precise Péclet numbers and therefore better models.

Bibliography

- [1] William E. Boyce and Richard C. DiPrima. *Elementary Differential Equations and Boundary Value Problems*. John Wiley & Sons, Inc., seventh edition, 2001.
- [2] Bayerisches Landesamt für Statistik und Datenverarbeitung [Bavarian State Office for Statistics and Data Processing]. Fortschreibung des bevölkerungsstandes, 2011.
- [3] Richard Habermann. *Elementary Applied Differential Equations, With Fourier Series and Boundary Value Problems*. Prentice Hall, third edition, 1998.
- [4] Gerald Katz. Environmental control technology development for geothermal energy. *Journal (Water Pollution Control Federation)*, 53(10):pp. 1447–1451, 1981.
- [5] Erika László. Geothermal energy: An old ally. *Ambio*, 10(5):pp. 248–249, 1981.
- [6] Phillip Wright. Geothermal energy: A sustainable resource of enormous potential. *JOM Journal of the Minerals, Metals and Materials Society*, 50:38–40, 1998. 10.1007/s11837-998-0305-7.

Appendix A

Matlab Source Code

A.1 eigens.m

```
clear all;

% Script to numerically compute eigenfunctions \phi for N modes.

N = input('Enter N: ');

% Basis eigenvalues.
mu = zeros(N,1);
for i = 1:N
    mu(i,1) = pi/2*(2*i-1);
end

% A diagonal matrix containing the basis eigenvalues.
M = diag(mu);

B = zeros(N,N);

% Use 'quad' function to compute integrals
% x is assumed to be a scalar
for i = 1:N
    for j = i:N
        B(i,j) = quad(@(x)(1-x.^2).*cos(mu(i).*x).*cos(mu(j).*x),0,1);
        B(j,i) = B(i,j); % cos(i)*cos(j) == cos(j)*cos(i)
    end
end

% Get eigenvalues and eigenvectors
% The i-th eigenvalue/eigenvector corresponds to the i-th eigenfunction(?)
```

```

[V,D] = eig(0.5*M,B);

% lambda is a column vector made out of the main diagonal of D (which
% contains the needed eigenvalues)
[lambda,ind] = sort(diag(D));

% Sort eigenvectors to correspond with their eigenvalues properly and
% normalize them to create matrix of coefficients.
c = V(:,ind);

for i = 1:N
    c(:,i) = c(:,i)/c(1,i);
end

% Eigenfunctions
phi = cell(N,1);
for i = 1:N
    phi{i} = @(x)sum(cos(mu.*x).*c(:,i));
end

% Numerically compute eigenfunctions
dx = 1/1000;
x = (0:dx:1)'; % length = 1/dx + 1

% The i-th column corresponds to the i-th eigenfunction
y = zeros(1/dx + 1,N);

for k = 1:N
    for l = 1:(1/dx + 1)
        y(l,k) = phi{k}(x(l));
    end
end
end

```

A.2 nondim.m

```

function [T,x,z,lambda] = nondim(N,L,Pe,Tg)
% Function to numerically compute values for the full model over N modes.

% Sets default values for variables.
if nargin < 4
    Tg = 1;
end
if nargin < 3
    Pe = 1000;
end
end

```

```

if nargin < 2
    L = 1;
end
if nargin == 0
    N = 10;
end

% Basis eigenvalues.
mu = zeros(N,1);
for i = 1:N
    mu(i,1) = pi/2*(2*i-1);
end

% A diagonal matrix containing the basis eigenvalues.
M = diag(mu);

B = zeros(N,N);

% Use 'quad' function to compute integrals
% x is assumed to be a scalar
for i = 1:N
    for j = i:N
        B(i,j) = quad(@(x)(1-x.^2).*cos(mu(i).*x).*cos(mu(j).*x),0,1);
        B(j,i) = B(i,j); % cos(i)*cos(j) == cos(j)*cos(i)
    end
end

% Get eigenvalues and eigenvectors
% The i-th eigenvalue/eigenvector corresponds to the i-th eigenfunction
[V,D] = eig(0.5*M,B);

% lambda is a column vector made out of the main diagonal of D (which
% contains the eigenvalues for \phi)
[lambda,ind] = sort(diag(D));

% Sort eigenvectors to correspond with their eigenvalues properly and
% normalize them to create matrix of coefficients.
c = V(:,ind);

for i = 1:N
    c(:,i) = c(:,i)/c(1,i);
end

% Eigenfunctions and amplitude functions.
phi = cell(N,1);
Z = cell(N,1);

```

```

for i = 1:N
    phi{i} = @(x)sum(cos(mu.*x).*c(:,i));
    Z{i} = @(z)exp(-lambda(i)./Pe.*z);
end

% Fourier coefficients
a = zeros(N,1);
for i = 1:N
    a(i) = Tg.*quad(@(x)sumcosc(x).*(1-x.^2),0,1);
end

% Sub-function for computing coefficients
function y = sumcosc(x)
    yy = 0;
    for ii = 1:N
        yy = yy + cos(mu(ii).*x).*c(ii,i);
    end
    y = yy;
end

% Numerically compute \Theta.
dx = 1/1000;
x = (0:dx:1)'; % Length = 1/dx + 1

dz = 1/1000;
z = (0:dz:L)'; % Length = L/dz + 1

Theta = zeros(1/dx + 1,L/dz + 1);

for k = 1:(L/dz + 1)
    for l = 1:(1/dx + 1)
        if mod(k,100) == 0 && l == 1
            k
        end
        Theta(l,k) = theta(x(l),z(k));
    end
end

% Subfunction for computing \Theta
function Thet = theta(x,z)
    TThet = 0;
    for ii = 1:N
        TThet = TThet + a(ii)*phi{ii}(x)*Z{ii}(z);
    end
    Thet = TThet;
end

```

```
end  
T = Theta;  
end
```